9-2009

Steady-Periodic Heating of a Cylinder

Kevin D. Cole
University of Nebraska - Lincoln, kcole1@unl.edu

Paul E. Crittenden
Jacksonville University, pcritte@ufl.edu

Steady-Periodic Heating of a Cylinder

Kevin D. Cole
Department of Mechanical Engineering,
University of Nebraska,
Lincoln, NE 68588-0656
e-mail: kcole1@unl.edu

Paul E. Crittenden
Department of Mathematics,
Jacksonville University,
Jacksonville, FL 32211
e-mail: pcritte@ju.edu

Steady periodic heating is an important experimental technique for measurement of thermal properties. In these methods the thermal properties are deduced from a systematic comparison between the data (such as temperature) and a detailed thermal model. This paper addresses steady-periodic heat transfer on cylindrical geometries with application to thermal-property measurements. The method of Green's functions is used to provide a comprehensive collection of exact analytical expressions for temperature in cylinders. Five kinds of boundary conditions are treated for one-, two-, and three-dimensional geometries. For some geometries an alternate form of the Green's function is given, which can be used for improvement of series convergence and for checking purposes to produce highly accurate numerical values. Numerical examples are given.
[DOI: 10.1115/1.3139107]

Keywords: frequency response, thermal transient, oscillating heat source, convective boundary, lumped boundary, surface-film boundary, extended surface

1 Introduction

Steady-periodic heat transfer in cylinders is important in several engineering applications including annular fins [1–3], rotating machinery such as electromagnetic bearings [4], and in devices experiencing periodic thermal contact such as engine exhaust valves [5].

In this paper, steady-periodic heat conduction in cylinders is presented with the method of Green's functions (GFs). This approach provides a comprehensive set of solutions and specific strategies for improving the numerical evaluation of these solutions.

There are several recent books on GF applied to heat conduction [6–8]. The book by Mandelis [9] is devoted exclusively to steady-periodic heat conduction with the method of GFs. Of the solutions given for cylindrical geometries, however, only three kinds of boundary conditions are treated, and only one form of the GF is given for each geometry.

The contributions of this paper are threefold. First, a great many steady-periodic solutions are presented systematically with the method of GFs for several cylindrical geometries. Second, five kinds of boundary conditions are treated in a unified fashion, two of which include a high-conductivity surface film. Many of these surface-film solutions have not been published before. Third, alternate forms of GFs are given for several geometries, which provide for efficient numerical computation and allow for independent verification that the numerical results are correct. Two geometries are studied in detail with numerical values computed from exact analytical solutions.

2 Steady-Periodic Relations

The steady-periodic temperature in cylindrical coordinates satisfies the following equations:

$$\frac{1}{r}\frac{\partial}{\partial r}\left(r\frac{\partial T}{\partial r}\right)+\frac{1}{r^2}\frac{\partial^2 T}{\partial \phi^2}+\frac{\partial^2 T}{\partial z^2}-\sigma^2 T=-\frac{1}{k}g(\boldsymbol{r},\omega) \quad \text{in domain } \Omega \tag{1}$$

$$k_i\frac{\partial T}{\partial n_i}+[h_i+j\omega(\rho c\epsilon)_i]T=f_i(\boldsymbol{r}_i,\omega) \quad \text{at boundary } i \tag{2}$$

where $\sigma^2=j\omega/\alpha$. Here complex-valued $T(\boldsymbol{r},\omega)$ is interpreted as the steady-periodic temperature (K) at vector location $\boldsymbol{r}$ and at a single frequency ω. The generalized boundary condition represents five types of boundary conditions depending on the choice of parameters k_i, h_i, and ϵ_i (the five kinds are (1) temperature, (2) flux, (3) convection, (4) surface film, and (5) surface film with convection). The boundary condition, Eq. (2), contains term $j\omega(\rho c\epsilon)_i T$, which represents heat storage in a surface film of thickness ϵ_i. Boundary conditions with a surface film, under steady-periodic conditions, are similar to convection boundary conditions, except that a complex quantity is added to the heat transfer coefficient. See Ref. [10] for further discussion of the steady-periodic heat equation and the five kinds of boundary conditions.

3 Green's Function Solution

The temperature will be found by the method of GF. Assume for the moment that the GF, symbol G, is known. Then the steady-periodic temperature is given by the following integral equation [6] (Chap. 3):

$$T(\boldsymbol{r},\omega)=\frac{\alpha}{k}\int g(\boldsymbol{r}',\omega)G(\boldsymbol{r},\boldsymbol{r}',\omega)dv'+\alpha\sum_i\int f_i(\boldsymbol{r}_i',\omega)\times\begin{bmatrix}-\partial G/\partial n_i' & \text{(first kind only)}\\ \frac{1}{k}G(\boldsymbol{r},\boldsymbol{r}_i',\omega) & \text{(second to fifth kinds)}\end{bmatrix}ds_i' \tag{3}$$

The first integral is the effect of internal heat generation g, and the second integral is the effect of each nonhomogeneous boundary term f_i. Note that the same GF appears in each integral but it is evaluated at locations appropriate for each integral.

The GF associated with Eqs. (1) and (2) is the response at $\boldsymbol{r}$ to a steady-periodic heat source located at $\boldsymbol{r}'$, and the GF satisfies

$$\nabla^2 G-\sigma^2 G=-\frac{1}{\alpha}\delta(\boldsymbol{r}-\boldsymbol{r}') \tag{4}$$

Contributed by the Heat Transfer Division of ASME for publication in the JOURNAL OF HEAT TRANSFER. Manuscript received May 28, 2008; final manuscript received March 26, 2009; published online June 22, 2009. Review conducted by Ofodike A. Ezekoye.

$$k_i \frac{\partial G}{\partial n_i} + \lambda_i G = 0 \quad \text{on boundary } i \tag{5}$$

Here $\lambda_i = h_i + j\omega(\rho c \epsilon)_i$ and $\delta(\mathbf{r}-\mathbf{r}')$ is the Dirac delta function. The coefficient $1/\alpha$ preceding the delta function in Eq. (4) provides for units of the steady-periodic GF that are consistent with earlier work [10]. The boundary conditions for the GF are homogeneous but of the same kind (see Ref. [6], Chap. 2) as for the temperature problem of interest. Thus, a different GF is needed for each geometry and for each combination of boundary conditions.

In Secs. 4–6, the method of GFs is applied to one-, two-, and three-dimensional cylinders. First, the GFs will be identified, and then temperature examples will be given.

4 Long Cylinder

In this section, we consider steady-periodic heating of an infinitely long cylinder. The heat conduction is along the radial direction only. The GF in this case satisfies the following equation:

$$\frac{\partial^2 G}{\partial r^2} + \frac{1}{r}\frac{\partial G}{\partial r} - \sigma^2 G = -\frac{1}{\alpha}\delta(r-r'), \quad a < r < b \tag{6}$$

Using variation of parameters, the solution may be found in the form

$$G(r|r') = \frac{1}{2\pi\alpha(1-A_1A_2)} \times \begin{Bmatrix} [A_2 I_0(\sigma r') + K_0(\sigma r')][I_0(\sigma r) + A_1 K_0(\sigma r)], & r < r' \\ [A_2 I_0(\sigma r) + K_0(\sigma r)][I_0(\sigma r') + A_1 K_0(\sigma r')], & r > r' \end{Bmatrix} \tag{7}$$

where

$$A_1 = \begin{cases} 0 & \text{if } a = 0 \text{ (solid cylinder)} \\ -\dfrac{I_0(\sigma a)}{K_0(\sigma a)} & \text{if kind 1 at } r = a \\ \dfrac{I_1(\sigma a)}{K_1(\sigma a)} & \text{if kind 2 at } r = a \\ \dfrac{k\sigma I_1(\sigma a) - \lambda_1 I_0(\sigma a)}{k\sigma K_1(\sigma a) + \lambda_1 K_0(\sigma a)} & \text{if kind 3, 4, or 5 at } r = a \end{cases} \tag{8}$$

and

$$A_2 = \begin{cases} 0 & b \to \infty \\ -\dfrac{K_0(\sigma b)}{I_0(\sigma b)} & \text{if kind 1 at } r = b \\ \dfrac{K_1(\sigma b)}{I_1(\sigma b)} & \text{if kind 2 at } r = b \\ \dfrac{k\sigma K_1(\sigma b) - \lambda_2 K_0(\sigma b)}{k\sigma I_1(\sigma b) + \lambda_2 I_0(\sigma b)} & \text{if kind 3, 4, or 5 at } r = b \end{cases} \tag{9}$$

The set of GFs given in Eq. (7) applies to 36 combinations of boundary conditions—six kinds at $r_{\min}$ and six at $r_{\max}$. This includes the zeroth kind to represent a nonphysical boundary at $r=0$ or $r \to \infty$. We use a numbering system to identify these GFs in the form *RIJ*, where *R* represents the radial coordinate, and $I,J = 0,1,\ldots,5$ represent the kinds of boundary condition present. For example, *R*11 denotes a hollow cylinder with type 1 boundaries. For more information on the numbering system, see Ref. [6] (Chap. 2).

5 Finite Cylinder With $T=T(r,z)$

Consider a finite-length hollow cylinder with outer radius b, inner radius a, and length L. This geometry can also describe a solid cylinder if $a=0$. Suppose the steady-periodic temperature in the finite cylinder does not depend on angle, then the temperature satisfies

$$\frac{1}{r}\frac{\partial}{\partial r}\left(r\frac{\partial T}{\partial r}\right) + \frac{\partial^2 T}{\partial z^2} - \sigma^2 T = -\frac{g(r,z,\omega)}{k} \tag{10}$$

and at the boundaries

$$k_i \frac{\partial T}{\partial n_i} + [h_i + j\omega(\rho c \epsilon)_i]T = f_i(r_i, z_i) \tag{11}$$

where $i=1$, 2, 3, and 4 represents boundaries at $r=a$, $r=b$, $z=0$, and $z=L$, respectively. Quantity ϵ_i is the thickness of a surface layer with high conductivity that may be present. The associated GF for the finite cylinder satisfies

$$\frac{1}{r}\frac{\partial}{\partial r}\left(r\frac{\partial G}{\partial r}\right) + \frac{\partial^2 G}{\partial z^2} - \sigma^2 G = -\frac{1}{\alpha}\delta(r-r')\,\delta(z-z') \tag{12}$$

and at the boundaries

$$k_i \frac{\partial G}{\partial n_i} + \lambda_i G = 0 \tag{13}$$

where $\lambda_i = h_i + j\omega(\rho c \epsilon)_i$.

The set of GFs given by Eqs. (12) and (13) represents a large number of geometries, with 36 combinations of boundary conditions along r and 36 combinations along z for a total of 1296 combinations. The number system for these GFs have the form *RIJZKL*, where *R* and *Z* represent the coordinate directions, and *I*, *J*, *K*, and *L* represent the types of boundary conditions present. For example, number *R*03*Z*33 represents a solid cylinder with convection (third kind) over the boundaries at $r=b$, $z=0$, and $z=L$.

There are two forms of the single-sum GF, one with eigenfunctions along the z-direction and the other with eigenfunction along the r-direction. Both are important, as one can be used to check the other, and where one converges slowly the other generally converges rapidly [11].

5.1 2D GF With Eigenfunctions Along *z*. The single-sum steady-periodic GF with eigenfunctions along the z-direction has the form

$$G(r,z|r',z',\omega) = \sum_{p=0}^{\infty} \frac{Z_p(z)Z_p(z')}{N_z(\nu_p)} Q_p(r,r') \tag{14}$$

where eigenfunctions Z_p satisfy

$$Z_n'' + \nu_p^2 Z_p = 0$$

along with boundary conditions at $z=0$ and $z=L$ drawn from those for G. Eigenfunctions Z_p, norm N_z, and eigenvalues ν_p are well-known values given in Table 1 (see also Refs. [11,12] (p. 35)).

Kernel function $Q_p(r,r')$ is identical with the 1D GF discussed earlier. That is,

$$Q_p(r,r') = G(r,r')|_{\sigma=\beta_p} \tag{15}$$

where $\beta_p^2 = \nu_p^2 + \sigma^2$.

5.2 2D GF With Eigenfunctions Along *r*. An alternate GF that satisfies Eq. (12) may also be constructed using eigenfunctions along the r direction. If the r-direction eigenfunctions are denoted $R_m(r)$, then the alternate single-sum GF may be written

$$G(r,z|r',z',\omega) = \sum_{m=0}^{\infty} \frac{R_m(r)R_m(r')}{N_r(\gamma_m)} P_m(z,z') \tag{16}$$

Eigenfunctions R_m satisfy

Table 1 Eigenfunctions along the *z*-direction. Note $B_1 = h_1 L/k$; $B_2 = h_2 L/k$. ((*a*) Eigenfunctions and (*b*) inverse norm and eigenvalues or conditions.)

Cases	$Z_p(z)$
	(*a*)
*Z*11, *Z*12, and *Z*13	$\sin(\nu_p z)$
*Z*21, *Z*22, and *Z*23	$\cos(\nu_p z)$
*Z*31, *Z*32, and *Z*33	$\nu_p L\cos(\nu_p z)+B_1\sin(\nu_p z)$

Case	$N_z(p)^{-1}$	ν_p or eigencondition
	(*b*)	
*Z*11	$2/L$	$p\pi/L$
*Z*12	$2/L$	$\dfrac{(2p-1)\pi}{2L}$
*Z*13[a]	$2D_p/L$	$\nu_p L\cot(\nu_p L)=-B_2$
*Z*21	$2/L$	$\dfrac{(2p-1)\pi}{2L}$
*Z*22	$\begin{cases}2/L, & \nu_p\neq 0\\ 1/L, & \nu_p=0\end{cases}$	$p\pi/L$
*Z*23[a]	$2D_p/L$	$\nu_p L\tan(\nu_p L)=B_2$
*Z*31	$\dfrac{2}{(\nu_p L)^2+B_1^2+B_1}$	$\nu_p L\cot(\nu_p L)=-B_1$
*Z*32	$\dfrac{2}{(\nu_p L)^2+B_1^2+B_1}$	$\nu_p L\tan(\nu_p L)=B_1$
*Z*33[b]	$2d_p/L$	$\tan(\nu_p L)=\dfrac{\nu_p L(B_1+B_2)}{(\nu_p L)^2-B_1B_2}$

[a] $D_p=[(\nu_p L)^2+B_2^2]/[(\nu_p L)^2+B_2^2+B_2]$.
[b] $d_p=D_p\div[(\nu_p L)^2+B_1^2+B_1D_p]$.

$$\frac{1}{r}\frac{\partial}{\partial r}\left(r\frac{\partial R_m}{\partial r}\right)-\gamma_m^2 R_m=0$$

along with the boundary conditions at $r=a$ and $r=b$. Eigenfunctions R_m have the form of Bessel functions of order zero. Eigenfunctions R_m and norm N_r are given in Table 2 (for $n=0$) and the conditions for computing eigenvalues γ_m are given in Table 3 for solid cylinders ($0<r<b$). For hollow cylinders see Ref. [12] (pp. 108–113) or Ref. [13].

Kernel function P_m is given by Ref. [10]:

$$P_m(z,z')=\frac{S_2^-(S_1^- e^{-\beta_m(2L-|z-z'|)}+S_1^+ e^{-\beta_m(2L-z-z')})}{2\alpha\beta_m(S_1^+S_2^+-S_1^-S_2^- e^{-2\beta_m L})}+\frac{S_2^+(S_1^+ e^{-\beta_m(|z-z'|)}+S_1^- e^{-\beta_m(z+z')})}{2\alpha\beta_m(S_1^+S_2^+-S_1^-S_2^- e^{-2\beta_m L})} \tag{17}$$

where $\beta_m^2=\gamma_m^2+\sigma^2$ and where subscripts 1 and 2 indicate sides $z=0$ and $z=L$ of the cylinder, respectively. Parameters S_M^+ and S_M^- depend on the boundary conditions on side M and are given by

$$S_M^+=\begin{cases}1 & \text{if side } M \text{ is kind 1 or kind 2}\\ \beta_m L+\mathrm{B}_M & \text{if side } M \text{ is kind 3, 4, or 5}\end{cases} \tag{18}$$

$$S_M^-=\begin{cases}-1 & \text{if side } M \text{ is kind 1}\\ 1 & \text{if side } M \text{ is kind 2}\\ \beta_m L-\mathrm{B}_M & \text{if side } M \text{ is kind 3, 4, or 5}\end{cases} \tag{19}$$

Here $\mathrm{B}_M=\lambda_M L/k$ is the Biot number for side M, and k is the conductivity of the cylinder.

Table 3 Eigenconditions for solid cylinders

Case	Eigencondition
*R*01	$J_n(\gamma_{nm}b)=0$
*R*02	$J_n'(\gamma_{nm}b)=0$
*R*03	$\gamma_{nm}bJ_n'(\gamma_{nm}b)+\mathrm{B}_2J_n(\gamma_{nm}b)=0$

6 Finite Cylinder With $T=T(r,\phi,z)$

In this section, the finite-length cylinder with three-dimensional heat conduction is treated. That is, temperature depends on spatial coordinates (r,ϕ,z). The steady-periodic temperature satisfies

$$\frac{1}{r}\frac{\partial}{\partial r}\left(r\frac{\partial T}{\partial r}\right)+\frac{1}{r^2}\frac{\partial^2 T}{\partial\phi^2}+\frac{\partial^2 T}{\partial z^2}-\sigma^2 T=-\frac{g(r,z,\omega)}{k} \tag{20}$$

and at the boundaries

$$k_i\frac{\partial T}{\partial n_i}+\lambda_i T=f_i(r_i,\phi_i,z_i) \tag{21}$$

where $i=1$, 2, 3, and 4 represents boundaries at $r=a$, $r=b$, $z=0$, and $z=L$, respectively.

The associated GF for 3D steady-periodic heat conduction in the finite cylinder satisfies

$$\frac{1}{r}\frac{\partial}{\partial r}\left(r\frac{\partial G}{\partial r}\right)+\frac{1}{r^2}\frac{\partial^2 G}{\partial\phi^2}+\frac{\partial^2 G}{\partial z^2}-\sigma^2 G=-\frac{1}{\alpha}\delta(r-r')\delta(z-z')\delta(\phi-\phi') \tag{22}$$

and at the boundaries

$$k_i\frac{\partial G}{\partial n_i}+\lambda_i G=0 \tag{23}$$

The set of GFs represented by Eqs. (22) and (23) represent 1296 combinations of boundary conditions (36 along r and 36 along z), denoted by GF number *RIJZKL*Φ00. Here Φ00 denotes the angular dependence for the full cylinder, and $I,J,K,L=0,1,\ldots,5$ denote the types of boundary conditions present. Two forms of the double-sum GF are discussed in Secs. 6.1 and 6.2.

Table 2 Eigenfunctions and norm for solid cylinders. Note $B_2=\lambda_2 b/k$.

Case	Condition at $r=b$	R_{nm}	$(N_r)^{-1}$ for $n\neq 0$	$(N_r)^{-1}$ for $n=0$
*R*01	$R_{nm}=0$	$J_n(\gamma_{nm}r)$	$\dfrac{2}{b^2J_n'(\gamma_{nm}b)}$	See $n\neq 0$
*R*02	$\dfrac{dR_{nm}}{dr}=0$	$J_n(\gamma_{nm}r)$	$\dfrac{2}{b^2J_n^2(\gamma_{nm}b)}\dfrac{b^2\gamma_{nm}^2}{(b^2\gamma_{nm}^2-n^2)}$	$\dfrac{2}{b^2}$
*R*03	$k\dfrac{dR_{nm}}{dr}+hR_{nm}=0$	$J_n(\gamma_{nm}r)$	$\dfrac{2}{b^2J_n^2(\gamma_{nm}b)}\dfrac{b^2\gamma_{nm}^2}{(B_2^2+b^2\gamma_{nm}^2-n^2)}$	See $n\neq 0$

6.1 3D GF With Eigenfunctions Along *z*. The double-sum steady-periodic GF with eigenfunctions along the z-direction has the form

$$G(r,\phi,z|r',\phi',z',\omega)=\sum_{n=0}^{\infty}\sum_{p=0}^{\infty}\frac{Z_p(z)Z_p(z')}{N_z(\nu_p)}\frac{\cos[n(\phi-\phi')]}{N_\phi}Q_{np}(r,r') \tag{24}$$

The boundary conditions at $z=0$ and $z=L$ are satisfied by the eigenfunctions in the z-direction, and the conditions at $\phi=0$ and $\phi=2\pi$ are satisfied by the eigenfunctions in the ϕ-direction. Here norm N_ϕ is equal to π for $n=0$ and 2π for $n\geq 1$.

Kernel function Q_{np} can be shown to have the form

$$Q_{np}(r|r')=\frac{1}{2\pi\alpha(1-A_1A_2)}\times\begin{Bmatrix}[A_2I_n(\beta_pr')+K_n(\beta_pr')][I_n(\beta_pr)+A_1K_n(\beta_pr)], & r<r'\\ [A_2I_n(\beta_pr)+K_n(\beta_pr)][I_n(\beta_pr')+A_1K_n(\beta_pr')], & r>r'\end{Bmatrix} \tag{25}$$

where

$$A_1=\frac{[\ \beta_paI_{n+1}(\beta_pa)+nI_n(\beta_pa))]-B_1I_n(\beta_pa)}{[\beta_paK_{n+1}(\beta_pa)-nK_n(\beta_pa)]+B_1K_n(\beta_pa)} \tag{26}$$

and

$$A_2=\frac{[\beta_pbK_{n+1}(\beta_pb)-nK_n(\beta_pb)]-B_2K_n(\beta_pb)}{[\beta_pbI_{n+1}(\beta_pb)+nI_n(\beta_pb)]+B_2I_n(\beta_pb)} \tag{27}$$

The quantities $B_1=\lambda_1a/k_1$ and $B_2=\lambda_2b/k_2$ are modified Biot numbers at the inner and outer radii, respectively. The above values for A_1 and A_2 are for the most general boundary condition (fifth kind). Values for other kinds of boundaries can be found by analogy with Eqs. (27)–(29). Some care is required when combining eigenfunctions Z_p and kernel functions Q_{np}, as they depend on different Biot numbers. In the finite-length cylinder, eigenfunctions Z_p depend on Biot numbers $B_M=\lambda_ML/k$, where λ_M is associated with the boundary conditions at $z=0$ and $z=L$. As many as four distinct Biot numbers may be present in the finite cylinder.

6.2 3D GF With Eigenfunctions Along *r*. An alternate GF that satisfies Eq. (22) may be constructed using eigenfunctions along the r-direction. If the r-direction eigenfunctions are denoted $R_{nm}(r)$, then the alternate double-sum GF may be written as

$$G(r,\phi,z|r',\phi',z',\omega)=\sum_{n=0}^{\infty}\sum_{m=0}^{\infty}\frac{R_{nm}(r)R_{nm}(r')}{N_r(\gamma_{nm})}\frac{\cos[n(\phi-\phi')]}{N_\phi}\times P_m(z,z') \tag{28}$$

The $m=0$ term of the series is needed only when zero is an eigenvalue (for cases *R*02 and *R*22). The series on n involves the functions $\cos[n(\phi-\phi')]$, which satisfy the periodic boundary conditions at $\phi=0$ and $\phi=2\pi$. The GF given above is similar in form to the real-valued *steady* GF published previously in Ref. [13]; however, for steady-periodic conditions considered here the eigenfunctions R_{nm}, norm N_r, and eigenvalues γ_{nm} can take on complex values. Eigenfunctions R_{nm} have the form of Bessel functions of order n and are listed in Table 2 along with their norms. The eigenconditions for γ_{nm} are listed in Table 3. For hollow cylinders, see Ref. [12] (Chap. 3). Note that the kernel function is identical to that discussed earlier in Eq. (17); however, here β_m is defined $\beta_m^2=\gamma_{nm}^2+\sigma^2$.

7 Temperature Examples

In the next two sections, numerical examples are given of the temperature in cylindrical geometries caused by steady-periodic heating. The first example is a cylinder heated at one end and experiencing axisymmetric convective heat loss from the other surfaces. The second example is a cylinder heated over a small region on its surface with convective heat loss.

8 Pin Fin With Heat Flux at Base

Steady-periodic heat transfer in fins has been studied several times [1–3]. Generally, a fin is long and thin and the temperature varies only along the axis of the fin; however, Kraus et al. [14] (Chap. 17) described the two-dimensional temperature in a rectangular fin with an oscillating base temperature. This example is concerned with a short cylindrical fin in which two-dimensional heat transfer is present. The base of the fin is uniformly heated by a steady-periodic heat flux, and the other surfaces are cooled by convection. This is geometry *R*03*Z*23. The temperature satisfies the following equations:

$$\frac{1}{r}\frac{\partial}{\partial r}\left(r\frac{\partial T}{\partial r}\right)+\frac{\partial^2T}{\partial z^2}-\sigma^2T=0 \tag{29}$$

$$\text{at } z=0,\quad -k\frac{\partial T}{\partial r}=q_0(\omega) \tag{30}$$

$$\text{at } z=L,\quad k\frac{\partial T}{\partial z}+hT=0 \tag{31}$$

$$\text{at } r=b,\quad k\frac{\partial T}{\partial r}+hT=0 \tag{32}$$

The temperature may be expressed as an integral involving the appropriate Green's function, as follows:

$$T(r,z,\omega)=\frac{\alpha}{k}\int_{r'=0}^{b}q_0G(r,z,\omega|r',z'=0)2\pi r'dr' \tag{33}$$

Mathematically, the temperature has a unique solution. However, there are two series forms of the GF that can provide two distinct series expressions for the temperature.

8.1 Eigenfunctions Along *z*. With eigenfunctions along the z-direction, the GF is given by

$$G(r,z|r',z'=0,\omega)=\sum_{p=1}^{\infty}\frac{Z_p(z)Z_p(0)}{N_z(\nu_p)}Q_p(r,r') \tag{34}$$

where the eigenfunction and norm are given by (Table 1)

$$Z_p(z)=\cos(\nu_pz) \tag{35}$$

$$\frac{1}{N_z(\nu_p)}=\frac{2}{L}\frac{(\nu_pL)^2+B_2^2}{(\nu_pL)^2+B_2^2+B_2} \tag{36}$$

where $B_2=hL/k$. Eigenvalues ν_p satisfy $\nu_pL\tan(\nu_pL)=hL/k$. The kernel function is given by

$$Q_p(r|r')=\frac{1}{2\pi\alpha}\begin{Bmatrix}[A_2I_0(\beta_pr')+K_0(\beta_pr')][I_0(\beta_pr)], & r<r'\\ [A_2I_0(\beta_pr)+K_0(\beta_pr)][I_0(\beta_pr')], & r>r'\end{Bmatrix} \tag{37}$$

where A_2 is given by

$$A_2=\frac{\beta_pLK_1(\beta_pb)-B_2K_0(\beta_pb)}{\beta_pLI_1(\beta_pb)+B_2I_0(\beta_pb)} \tag{38}$$

and where $\beta_p^2=\nu_p^2+\sigma^2$. Replace this GF into the temperature integral, Eq. (33), and evaluate the integral over r' to find

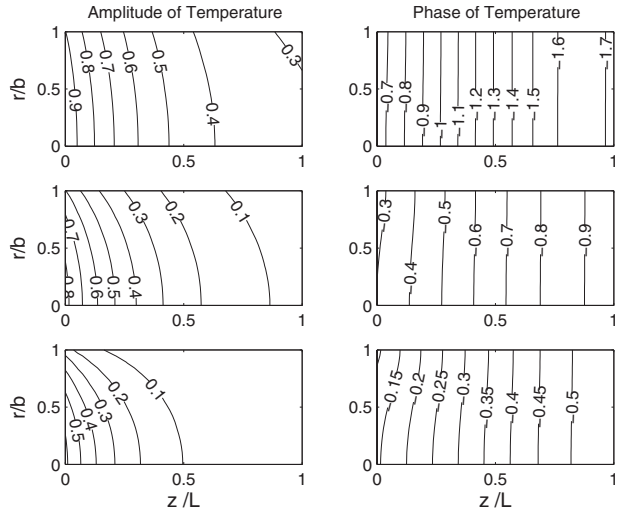

Fig. 1 Effect of varying convection on the amplitude and phase of the temperature in a cylinder of aspect ratio $b/L=0.5$. The cylinder is heated at $z=0$ and cooled by convection at $r/b=1$ and $z/L=1$. The heating frequency is fixed at $\omega b^2/\alpha=1.0$ and the boundary convection is given by $hb/k=0.2$, 1.0, and 5.0 for the top, middle, and bottom of the figure, respectively.

$$\frac{T(r,z,\omega)}{q_0 b/k}=\sum_{p=1}^{\infty}\cos(\nu_p z)\frac{2b}{L}\frac{(\nu_p L)^2+B_2^2}{(\nu_p L)^2+B_2^2+B_2}\times\left\{\frac{1}{\beta_p b}[A_2 I_1(\beta_p b)-K_1(\beta_p b)]I_0(\beta_p r)+\frac{1}{\beta_p^2 b^2}\right\} \tag{39}$$

8.2 Eigenfunctions Along *r*. An alternate form of the GF has eigenfunctions along the r-direction, and is given by

$$G(r,z|r',z'=0,\omega)=\sum_{m=1}^{\infty}\frac{R_m(r)R_m(r')}{N_r(\gamma_m)}P_m(z,z'=0) \tag{40}$$

where the eigenfunction and norm are given by (Table 2)

$$R_m(r)=J_0(\gamma_m r) \tag{41}$$

$$\frac{1}{N_r}=\frac{2}{J_0^2(\gamma_m b)}\frac{\gamma_m^2}{[\,(hb/k)^2+b^2\gamma_m^2)]} \tag{42}$$

where eigenvalue γ_m satisfies (Table 3)

$$\gamma_m b J_0'(\gamma_m b)+B_2 J_0(\gamma_m b)=0 \tag{43}$$

Kernel function P is given by Eq. (17) for a type 2 boundary at $z=0$ and a type 3 boundary at $z=L$ (case $Z23$):

$$P(z,z'=0)=\frac{S_2^- e^{-\beta_m(2L-z)}+S_2^+ e^{-\beta_m z}}{\beta_m(S_2^+-S_2^- e^{-2\beta_m L})} \tag{44}$$

where $\beta_m^2=\gamma_m^2+\sigma^2$, $S_2^+=\beta_m L+hL/k$, and $S_2^-=\beta_m L-hL/k$. This form of the GF may be substituted into the temperature integral to find an alternate series expression for the temperature

$$\frac{T(r,z,\omega)}{q_0 b/k}=\sum_{m=1}^{\infty}\frac{1}{\gamma_m b}J_0(\gamma_m r)J_1(\gamma_m b)\frac{2\gamma_m^2 b^2}{J_0^2(\gamma_m b)[(hb/k)^2+b^2\gamma_m^2]}\times\frac{(\beta_m L-hL/k)e^{-\beta_m(2L-z)}+(\beta_m L+hL/k)e^{-\beta_m z}}{\beta_m b[(\beta_m L+hL/k)-(\beta_m L-hL/k)e^{-2\beta_m L}]} \tag{45}$$

Numerical values for the temperature in the pin fin were computed using both temperature series, Eqs. (39) and (45), and the results agree to five significant figures, providing a very strong check on the correctness of the results. As both series are exact, closer agreement could have been secured by including more terms in the truncated sum. In Fig. 1, the contour plots of the amplitude and phase of the temperature are given for a fin of aspect ratio $b/L=0.5$. The frequency is fixed at $\omega b^2/\alpha=1.0$ and the results for Biot number $hb/k=0.2$, 1.0, and 5.0 are shown at the top, middle, and bottom of the figure, respectively. The amplitude of the temperature is largest where the heat is added ($z=0$) and decreases along the length of the fin. Heat leaves the fin along the $r/b=1$

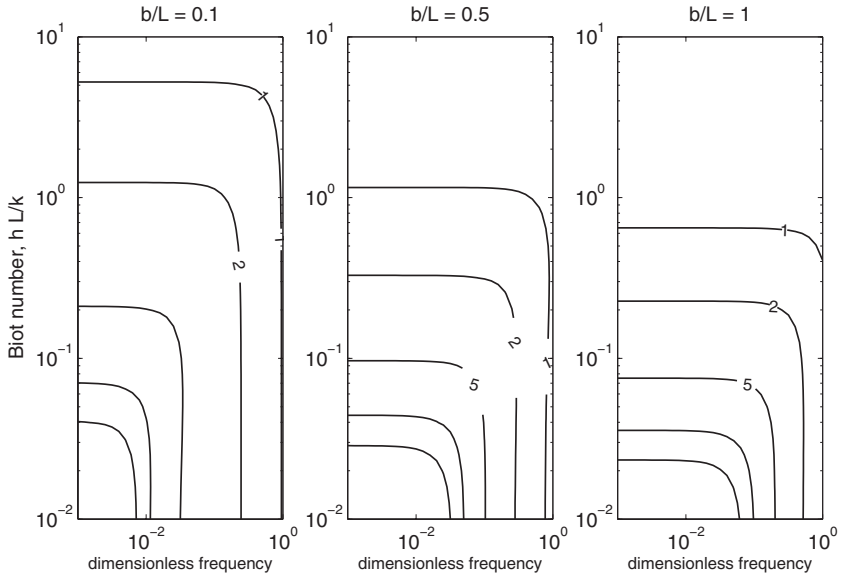

Fig. 2 Fin effectiveness in the pin fin heated at the base ($z=0$) as a function of Biot number and dimensionless frequency $\omega b^2/\alpha$ for aspect ratios $b/L=0.1$, 0.5, and 1.0

boundary, demonstrated by the slope of the temperature at the boundary, which is proportional to heat flux. Thus, as the Biot number increases, the slope at the boundary increases along with the boundary heat flux.

The phase of the temperature shown in Fig. 1 is negative and closest to zero at the heating location $z=0$. As z increases, the phase becomes more negative (moving further from zero). For the smallest Biot number (at the top of the figure), the change in phase along the fin is most pronounced, and as the Biot number increases there is less change in phase along the fin.

In Fig. 2, the effectiveness of fins with three different aspect ratios are graphed as a function of the Biot number hL/k and the dimensionless frequency $\omega b^2/\alpha$. The fin effectiveness (also called the fin-removal number) is defined as the conductive heat flow into the base of the fin divided by the convective heat flow through the fin-base area if the fin was not present [14] (p. 92). The total flow into the fin was calculated by differentiating the temperature expressions (at $z=0$) term by term and then integrating over the cross sectional area. A fin is usually considered justifiable if the effectiveness is greater than or equal to 2. At low frequencies, for a fixed aspect ratio, the fin is more effective at lower Biot numbers as expected. As frequency increases, the fin becomes less effective due to the insufficient time between the fluctuations for the heat to transfer down the fin. It is also interesting to note that thinner fins are more effective at lower frequencies but this is not necessarily true at higher frequencies. For example, a fin with a Biot number of 10^{-2}, an aspect ratio of 1, and an effectiveness of 2 would have an effectiveness somewhat less than 2 if the aspect ratio was changed to 0.1 while holding all of the other parameters constant.

9 Solid Cylinder Heated Over a Sector of Its Surface and Cooled by Convection

Consider a solid cylinder with steady-periodic heating over an angular sector of the curved surface, parallel to the cylinder axis, and cooled by convection over the entire curved surface. The flat ends of the cylinder are fixed at the fluid temperature. This geometry is an approximate thermal model of a hot-film sensor used to measure fluid flow. The temperature satisfies the following equations:

$$\frac{1}{r}\frac{\partial}{\partial r}\left(r\frac{\partial T}{\partial r}\right)+\frac{1}{r^2}\frac{\partial^2 T}{\partial \phi^2}+\frac{\partial^2 T}{\partial z^2}-\sigma^2 T+\frac{g(r,\phi,z)}{k}=0 \tag{46}$$

$$\text{at } z=0, \quad T=T_\infty \tag{47}$$

$$\text{at } z=L, \quad T=T_\infty \tag{48}$$

$$\text{at } r=b, \quad k\frac{\partial T}{\partial r}+hT=hT_\infty \tag{49}$$

The heating function is given by

$$g(r,\phi,z)=\begin{cases} q_0\delta(r-b) & 0<\phi<\phi_0 \\ 0 & \phi_0<\phi<2\pi \end{cases} \tag{50}$$

Note that the heat is introduced at surface $r=b$. This is geometry $R03Z11\Phi00$ in the heat conduction numbering system. The temperature may be stated in the form of an integral with the GF, as follows:

$$T(r,\phi,z,\omega)-T_\infty=\frac{\alpha}{k}\int_{\phi'=0}^{\phi_0}\int_{z'=0}^{L} q_0 \times G(r,\phi,z,\omega|r'=b,\phi',z')dz'd\phi' b \tag{51}$$

There are two forms of the GF that allow for two distinct series expressions for the temperature.

9.1 Eigenfunctions Along *z*. With eigenfunctions along the z-direction, the GF is given by Eq. (24). The eigenfunction and norm are given by Table 2 (case $Z11$) and the kernel function is given by Eq. (25) (for case $R03$). Replace the GF into the temperature integral, Eq. (51), and evaluate the integrals on ϕ' and z':

$$\frac{T(r,\phi,z)-T_\infty}{q_0 b/k}=\sum_{p=1}^{\infty}\sum_{n=0}^{\infty}\frac{2\sin(p\pi z/L)[1-(-1)^p]}{p\pi} \times C_n[A_2(n)I_n(\beta_p b)+K_n(\beta_p b)]\frac{I_n(\beta_p r)}{2\pi} \tag{52}$$

where

$$C_n=\begin{cases} \phi_0/\pi, & n=0 \\ \{\sin(n\phi)-\sin n(\phi-\phi_0)\}/(2\pi n), & n\neq 0 \end{cases}$$

and where

$$A_2(n)=\frac{[\beta_p bK_{n_+1}(\beta_p b)-nK_n(\beta_p b)]-B_2K_n(\beta_p b)}{[\beta_p bI_{n+1}(\beta_p b)+nI_n(\beta_p b)]+B_2I_n(\beta_p b)} \tag{53}$$

with $B_2=hb/k$. Note that the integral over ϕ' must be treated separately when $n=0$.

9.2 Eigenfunctions Along *r*. An alternate form of the GF, with eigenfunctions along the r-direction, is given by Eq. (28). The eigenfunction and norm are given by case $R03$ in Table 3, and the kernel function P_m is given by Eq. (17), with $\beta^2=\gamma_{nm}^2+\sigma^2$. Replace the alternate GF into the integral expression for the GF and evaluate the integrals over ϕ' and z' to find the an alternate series expression for the temperature

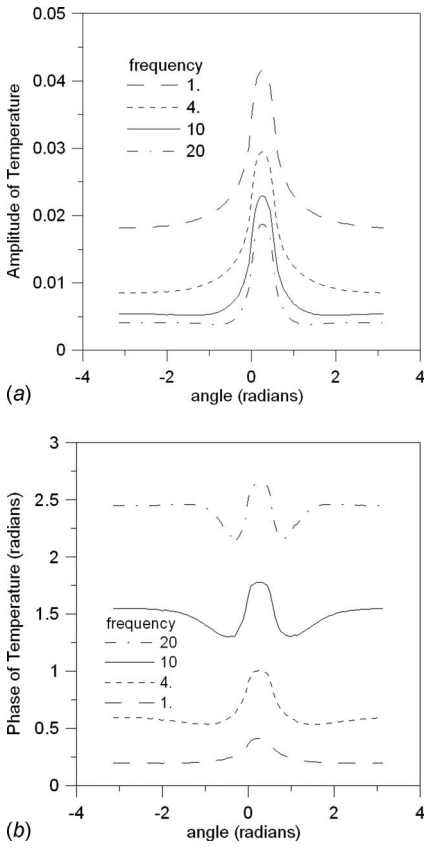

Fig. 3 Amplitude and phase of the temperature around the circumference of a cylinder ($r=b$, $z=L/2$) for several values of the (dimensionless) heating frequency. The cylinder surface is heated steady periodically over a small strip $0<\phi<0.2$ and the convection on the curved surface is characterized by $B_2=1$.

$$\frac{T(r,\phi,z)-T_\infty}{q_0 b/k}=\sum_{m=1}^{\infty}\sum_{n=0}^{\infty}J_n(\gamma_{nm}r)\frac{2\gamma_{nm}^2}{J_n(\gamma_{nm}b)(hb/k)^2+b^2\gamma_{nm}^2-n^2)}\times C_n\left[\frac{1}{\beta^2}+\frac{e^{-\beta(2L-z)}-e^{-\beta(L-z)}-e^{-2\beta L}-e^{-\beta z}}{\beta^2(1-e^{-2\beta L})}\right] \tag{54}$$

where C_n is given above. Note that additive term $1/\beta^2$, from integration on z' of the kernel function, may cause slow series convergence because this portion of the series does not contain a convergence-promoting exponential function. The series containing this additive term can be shown to correspond to a two-dimensional temperature distribution that does not depend on coordinate z and it can be replaced by a faster-converging single-sum form (see Ref. [11]).

Numerical values were computed for the amplitude and phase of the dimensionless temperature on the cylinder surface $r=b$ and at the midpoint $z=L/2$. The heated strip is located on $0<\phi<0.2$ and the aspect ratio of the cylinder is $b/L=0.2$.

Figure 3 shows the temperature amplitude and phase at the spatial location ($r=b$, $z=L/2$), with several different heating frequencies and the Biot number is fixed at $B_2=1$. The temperature amplitude decreases as the frequency increases, also the temperature becomes more localized to the heater at higher frequencies. As an explanation, there is less time for angular heat diffusion at higher frequencies. For all frequencies, the phase contains a flat region far from the heater; however, the level of this flat region increases with increasing frequency.

10 Summary

In this paper, a family of solutions to steady-periodic heating in cylinders has been presented with the method of Green's functions. Five types of boundary conditions have been treated. Solutions are given for cylinder geometries described by one, two, and three spatial coordinates, along with numerical examples. For some geometries alternate forms of the GF are given, which can be used for checking purposes and for improving the convergence behavior of the resulting temperature solutions. One application of these steady-periodic heat conduction solutions is for use with inverse methods for determining thermal properties from experimental temperature data.

Nomenclature

a = inner radius (m)
b = outer radius (m)
B_i = Biot number at boundary i
f_i = known effect at boundary i
g = internal heating at frequency ω
G = steady-periodic Green's function
h_i = heat transfer coefficient (W m^{-2} K^{-1})
i = index
I_n = modified Bessel function, order n
j = imaginary number, $\sqrt{-1}$
k = thermal conductivity (W m^{-1} K^{-1})
K_n = modified Bessel function, order n
L = length of domain in z-direction (m)
m = index
n = index
n_i = outward-facing unit normal vector on boundary i
N = norm
p = index
P = kernel function along z direction
q = steady-periodic heat flux (W m^{-2})
Q = kernel function along r direction
r = radial coordinate
R = eigenfunction along r-direction
S_M = coefficient for kernel function P
t = time (s)
T = steady-periodic temperature (K)
z = axial coordinate
Z_p = eigenfunction along z-direction

Greek Symbols

α = thermal diffusivity (m^2 s^{-1})
β = parameter for kernel function
δ = Dirac delta function
ϵ = thickness of surface layer on boundary
γ = eigenvalue associated with R
λ = boundary parameter, type 3, 4, or 5
ν_p = eigenvalue associated with Z_p
ρ = density (kg m^{-3})
σ = $[j\omega/\alpha]^{1/2}$
ϕ = angular coordinate (rad)
ω = frequency (rad s^{-1})

References

[1] Aziz, A., and Sofrata, H., 1981, "Fin Performance in an Oscillating Temperature Environment," Appl. Energy, **9**, pp. 13–21.
[2] Houghton, J. M., Ingham, D. B., and Heggs, P. J., 1992, "The One-Dimensional Analysis of Oscillatory Heat Transfer in a Fin Assembly," ASME J. Heat Transfer, **114**, pp. 548–552.
[3] Wu, S., Shiu, C. L., and Wu, W. J., 1996, "Analysis on Transient Heat Transfer in Annular Fins of Various Shapes With Their Bases Subjected to a Heat Flux Varying as a Sinusoidal Time Function," Comput. Struct., **61**(4), pp. 725–734.
[4] Jones, G. F., and Natarj, C., 1997, "Heat Transfer in an Electromagnetic Bearing," ASME J. Heat Transfer, **119**(3), pp. 611–616.
[5] Paradis, I., Wagner, J. R., and Marotta, E. E., 2002, "Thermal Periodic Contact of Exhaust Valves in Spark-Ignition Air-Cooled Engines," J. Thermophys. Heat Transfer, **16**(3), pp. 356–365.
[6] Beck, J. V., Cole, K. D., Haji-Sheikh, A., and Litkouhi, B., 1992, *Heat Conduction Using Green's Functions*, Hemisphere, New York.
[7] Duffy, D. G., 2001, *Green's Functions With Applications*, Chapman and Hall, London/CRC, Boca Raton, FL.
[8] Melnikov, Y. A., 1999, *Influence Functions and Matrices*, Dekker, New York.
[9] Mandelis, A., 2001, *Diffusion-Wave Fields, Mathematical Methods and Green's Functions*, Springer, New York.
[10] Cole, K. D., 2006, "Steady-Periodic Green's Functions and Thermal-Measurement Applications in Rectangular Coordinates," ASME J. Heat Transfer, **128**, pp. 709–716.
[11] Crittenden, P. E., and Cole, K. D., 2002, "Fast-Converging Steady-State Heat Conduction in a Rectangular Parallelepiped," Int. J. Heat Mass Transfer, **45**, pp. 3585–3596.
[12] Ozisik, M. N., 1993, *Heat Conduction*, Wiley, New York.
[13] Cole, K. D., 2004, "Fast-Converging Series for Steady Heat Conduction in the Circular Cylinder," J. Eng. Math., **49**, pp. 217–232.
[14] Kraus, A. D., Aziz, A., and Welty, J., 2001, *Extended Surface Heat Transfer*, Wiley, New York.